

Numerical Discrete-Time Implementation of Continuous-Time Linear-Quadratic Model Predictive Control

Zhanhao Zhang, Anders Hilmar Damm Christensen, Steen Hørsholt, John Bagterp Jørgensen

Abstract—This study presents the design, discretization and implementation of the continuous-time linear-quadratic model predictive control (CT-LMPC). The control model of the CT-LMPC is parameterized as transfer functions with time delays, and they are separated into deterministic and stochastic parts for relevant control and filtering algorithms. We formulate time-delay, finite-horizon CT linear-quadratic optimal control problems (LQ-OCPs) for the CT-LMPC. By assuming piece-wise constant inputs and constraints, we present the numerical discretization of the proposed LQ-OCPs and show how to convert the discrete-time (DT) equivalent into a standard quadratic program. The performance of the CT-LMPC is compared with the conventional DT-LMPC algorithm. Our numerical experiments show that, under fixed tuning parameters, the CT-LMPC shows better closed-loop performance as the sampling time increases than the conventional DT-LMPC.

I. INTRODUCTION

Consider the following continuous-time (CT) linear-quadratic optimal control problem (LQ-OCP) for the linear model predictive control (LMPC)

$$\min \phi = \int_{t_0}^{t_0+T} l(\bar{z}(t)) dt \quad (1a)$$

$$\text{s.t. } x(t_0) = \hat{x}_0, \quad (1b)$$

$$u(t) = u_k, \quad t_k \leq t < t_{k+1}, k \in \mathcal{N}, \quad (1c)$$

$$\dot{x}(t) = A_c x(t) + B_c u(t), \quad t_0 \leq t < t_0 + T, \quad (1d)$$

$$z(t) = C_c x(t) + D_c u(t), \quad t_0 \leq t < t_0 + T, \quad (1e)$$

$$\bar{z}(t) = \bar{z}_k, \quad t_k \leq t < t_{k+1}, k \in \mathcal{N}, \quad (1f)$$

$$\bar{z}(t) = z(t) - \bar{z}(t), \quad t_0 \leq t < t_0 + T, \quad (1g)$$

with the stage cost function

$$l_c(\bar{z}(t)) = \frac{1}{2} \|W_z \bar{z}(t)\|_2^2 = \frac{1}{2} (\bar{z}(t)' Q_c \bar{z}(t)), \quad (2)$$

where $x \in \mathbb{R}^{n_x \times 1}$ is the state, $u \in \mathbb{R}^{n_u \times 1}$ is the input, $z \in \mathbb{R}^{n_z \times 1}$ and $\bar{z} \in \mathbb{R}^{n_z \times 1}$ are the output and its reference. $Q_c = W_z' W_z$ is semi-positive definite weight matrix. $T = NT_s$ is the control horizon and $\mathcal{N} = 0, 1, \dots, N-1$.

In (1), we are assuming piece-wise constant inputs (1c) and reference (1f) since most control systems in real-world scenarios operate on digital platforms. The corresponding discrete-time (DT) equivalent is

$$\min_{x,u} \phi = \sum_{k \in \mathcal{N}} l_k(x_k, u_k) \quad (3a)$$

$$\text{s.t. } x_0 = \hat{x}_0, \quad (3b)$$

$$x_{k+1} = Ax_k + Bu_k, \quad k \in \mathcal{N}, \quad (3c)$$

with the stage costs

$$l_k(x_k, u_k) = \frac{1}{2} \begin{bmatrix} x_k \\ u_k \end{bmatrix}' Q \begin{bmatrix} x_k \\ u_k \end{bmatrix} + q_k' \begin{bmatrix} x_k \\ u_k \end{bmatrix} + \rho_k, \quad k \in \mathcal{N}, \quad (4)$$

where Q is a symmetric positive semi-definite matrix and

$$Q = \begin{bmatrix} Q_{xx} & Q_{xu} \\ Q_{ux} & Q_{uu} \end{bmatrix}, \quad q_k = \begin{bmatrix} q_{x,k} \\ q_{u,k} \end{bmatrix}. \quad (5)$$

The LQ-OCP is considered one of the fundamental problems in optimal control theory. This class of problems capture plenty of attention due to their simplicity and mathematical tractability. There is abundant research on the solution and discretization methods of optimal control problems described in (1) and (3). Most studies consider piece-wise constant inputs and use numerical discretization methods (e.g., Euler and Runge-Kutta methods) to obtain the DT equivalent and derive the solution [1], [4], [6], [9], [20]. In [2], [3], [5], authors explored the discrete equivalent of the LQ-OCP (1) and described the analytic expressions of the desired equivalent, discrete weighting matrices Q and q_k described in (5).

On the other hand, model predictive control, which might be the most successful advanced control algorithm in the industry, has a strong connection with the LQ-OCP. This relationship arises from using the LQ-OCP as the underlying optimization problem within the MPC framework. However, due to the consideration of computational efficiency and ease of implementation, almost all LMPC applications implemented in practice use DT models and diagonal weight matrices rather than the discrete weight matrix Q described in (5). In principle, non-diagonal weight matrices can be used. However, this is almost infeasible in practice as it will significantly increase the complexity of tuning. The previous studies [16], [17] proposed a novel computational procedure for input-constrained CT linear-quadratic regulator problem (LQR) with an infinite horizon. They pointed out that the discrete weight matrix Q can be computed with one exponential matrix instead of standard numerical discretization methods, and the numerical experiments showed that the CT LQR offers significant advantages over the DT MPC. Some other interesting results about the CT LQR or CT MPC can be found in [12], [13], [21].

However, the existing literature has not investigated the case with time delays, which is common in real-world scenarios (e.g., the system model is a MIMO transfer function with time delays). Therefore, in this paper, we would like to investigate the CT linear-quadratic model

predictive control (CT-LMPC) and compare it with the standard DT-LMPC. This paper focuses on the following problems:

1. *The numerical discretization of CT LQ-OCPs subject to linear time-delay systems*
2. *The numerical discrete-time implementation of CT-LMPC*

This paper is organized as follows. Section II introduces the control model and different objective functions of the CT-LMPC and present their discretization and implementation. Section III presents numerical experiments comparing and testing the proposed CT-LMPC and conventional DT-LMPC. The conclusions are given in Section IV.

II. DISCRETIZATION OF CT-LMPC

This section describes the discretization of linear time-delay models and the LQ-OCPs for the CT-LMPC.

A. Discretization of linear time-delay models

Consider a MIMO input-output model

$$\mathbf{Z}(s) = G(s)U(s) + H(s)W(s), \quad (6a)$$

$$\mathbf{Y}(s) = \mathbf{Z}(s) + \mathbf{V}(s), \quad (6b)$$

with the deterministic and stochastic transfer functions $G(s)$ and $H(s)$

$$G(s) = \begin{bmatrix} g_{11}(s) & \cdots & g_{1n_u}(s) \\ \vdots & \ddots & \vdots \\ g_{n_z1}(s) & \cdots & g_{n_z n_u}(s) \end{bmatrix}, \quad g_{ij}(s) = \frac{b_{ij}(s)}{a_{ij}(s)} e^{-\tau_{ij}s}, \quad (7a)$$

$$H(s) = \begin{bmatrix} h_{11}(s) & \cdots & h_{1n_w}(s) \\ \vdots & \ddots & \vdots \\ h_{n_z1}(s) & \cdots & h_{n_z n_w}(s) \end{bmatrix}, \quad h_{ip}(s) = \frac{d_{ip}(s)}{c_{ip}(s)}, \quad (7b)$$

where U and W are the deterministic and stochastic inputs to the system. Z and Y are the output and measurement and V indicates the measurement noise. We assume that $g_{ij}(s)$ for $i = 1, 2, \dots, n_z$, $j = 1, 2, \dots, n_u$ with the input time delay $\{\tau_{ij}\} \in \mathbb{R}_0^+$ is proper, and $h_{ip}(s)$ for $p = 1, 2, \dots, n_w$ is strictly proper and has no time delay.

Based on [8], using

$$\mathbf{Z}^d(s) = G(s)U(s), \quad \mathbf{Z}^s(s) = H(s)W(s), \quad (8)$$

and $\mathbf{Z}(s) = \mathbf{Z}^d(s) + \mathbf{Z}^s(s)$, the Noise-Separation (NS) state space realization of (6) can be performed as

$$\mathbf{Z}^d(s) \sim \begin{cases} \dot{x}_{ij}^d(t) = A_{c,ij}^d x_{ij}^d(t) + B_{c,ij}^d u_j(t - \tau_{ij}), \\ z_{ij}^d(t) = C_{c,ij}^d x_{ij}^d(t) + D_{c,ij}^d u_j(t - \tau_{ij}), \end{cases} \quad (9a)$$

$$\mathbf{Z}^s(s) \sim \begin{cases} d\mathbf{x}^s(t) = A_c^s \mathbf{x}^s(t) dt + B_c^s d\boldsymbol{\omega}(t), \\ \mathbf{z}^s(t) = C_c^s \mathbf{x}^s(t), \quad d\boldsymbol{\omega}(t) \sim N_{iid}(0, Idt), \end{cases} \quad (9b)$$

with the system variables

$$\mathbf{x}^d = [x_{11}^d \quad x_{21}^d \quad \cdots \quad x_{n_z n_u}^d]', \quad \mathbf{z}_i^d(t) = \sum_{j=1}^{n_u} z_{ij}^d(t), \quad (10a)$$

$$\mathbf{z}^d = [z_1^d \quad z_2^d \quad \cdots \quad z_{n_z}^d]', \quad \mathbf{z}(t) = \mathbf{z}^d(t) + \mathbf{z}^s(t), \quad (10b)$$

where we convert the deterministic part $Z^d(s)$ into $[i \times j]$ SISO time-delay state space models as they have different time delays and cannot be expressed by one standard state space model. Note that $\mathcal{G}_c = \{A_{c,ij}^d, B_{c,ij}^d, C_{c,ij}^d, D_{c,ij}^d\}$ and $\mathcal{H}_c = \{A_c^s, B_c^s, C_c^s\}$ are deterministic and stochastic system matrices.

The corresponding discrete-time state space models are

$$\mathbf{Z}^d(s) \sim \begin{cases} x_{k+1}^d = A^d x_k^d + B^d u_k, \\ z_k^d = C^d x_k^d + D^d u_k, \end{cases} \quad (11a)$$

$$\mathbf{Z}^s(s) \sim \begin{cases} \mathbf{x}_{k+1}^s = A^s \mathbf{x}_k^s + \mathbf{w}_k, \\ \mathbf{z}_k^s = C^s \mathbf{x}_k^s, \end{cases} \quad (11b)$$

and

$$\mathbf{y}_k = \mathbf{z}_k + \mathbf{v}_k, \quad \begin{bmatrix} \mathbf{w}_k \\ \mathbf{v}_k \end{bmatrix} \sim N_{iid} \left(\begin{bmatrix} 0 \\ 0 \end{bmatrix}, \begin{bmatrix} R_{ww} & 0 \\ 0 & R_{vv} \end{bmatrix} \right), \quad (12)$$

where the deterministic system (11a) are obtained by stacking the all SISO deterministic state space models [22]. Note that $\mathcal{G}_d = \{A^d, B^d, C^d, D^d\}$ and $\mathcal{H}_d = \{A^s, C^s\}$ are corresponding discrete system matrices.

The covariance $R_{ww} = \int_0^{T_s} e^{A_c^s t} B_c^s B_c^{s'} e^{A_c^s t'} dt$ can be solved using ordinary differential equation (ODE) methods or by $\begin{bmatrix} \Phi_{11} & \Phi_{12} \\ 0 & \Phi_{21} \end{bmatrix} = \exp \left(\begin{bmatrix} -A_c^s & B_c^s B_c^{s'} \\ 0 & A_c^s \end{bmatrix} \right)$ and $R_{ww} = \Phi'_{22} \Phi_{12}$.

The main advantage of using the NS state space realization is one may run the filtering with (9b) and run the control algorithm with (9a). The Kalman filter for (11b) can be performed as

$$\hat{\mathbf{y}}_{k|k-1}^s = C^s \hat{\mathbf{x}}_{k|k-1}^s, \quad e_k = \mathbf{y}_k^s - \hat{\mathbf{y}}_{k|k-1}^s, \quad (13a)$$

$$\hat{\mathbf{x}}_{k|k}^s = \hat{\mathbf{x}}_{k|k-1}^s + K_{fx} e_k, \quad (13b)$$

with the measurement covariance and the Kalman gain

$$R_e = C^s P (C^s)' + R_{ww}, \quad K_{fx} = P (C^s)' R_e^{-1}, \quad (13c)$$

where P indicates the stationary state error covariance obtained by the solution of discrete-time Algebraic Riccati Equation (DARE)

$$P = A^s P (A^s)' - A^s P (C^s)' R_e^{-1} C^s P (A^s)' + R_{vv}. \quad (14)$$

We then could obtain the following prediction expressions

$$\hat{x}_{k+j+1|k}^d = A^d \hat{x}_{k+j|k}^d + B^d u_{k+j}, \quad \hat{x}_{k+j+1|k}^s = A^s \hat{x}_{k+j|k}^s, \quad (15a)$$

$$\hat{z}_{k+j|k}^d = C^d \hat{x}_{k+j|k}^d + D^d u_{k+j}, \quad \hat{z}_{k+j|k}^s = C^s \hat{x}_{k+j|k}^s, \quad (15b)$$

$$\hat{z}_{k+j|k} = \hat{z}_{k+j|k}^d + \hat{z}_{k+j|k}^s, \quad \text{for } j = 1, \dots, N. \quad (15c)$$

Remark 1 The NS state space expressions (9) corresponding to the linear stochastic differential equation (SDE) model

$$d\mathbf{x}(t) = (A_c \mathbf{x}(t) + B_c u(t - \tau)) dt + G_c d\boldsymbol{\omega}(t), \quad (16a)$$

$$\mathbf{z}(t) = C_c \mathbf{x}(t) + D_c u(t - \tau), \quad (16b)$$

where $\mathbf{x} = [x^d, x^s]$ and $\mathbf{x} \sim N(\hat{x}_0, P_0)$ and

$$A_c = \begin{bmatrix} A_c^d & 0 \\ 0 & A_c^s \end{bmatrix}, \quad B_c = \begin{bmatrix} B_c^d \\ 0 \end{bmatrix}, \quad G_c = \begin{bmatrix} 0 \\ B_c^s \end{bmatrix}, \quad (16c)$$

$$C = \begin{bmatrix} C^d & C^s \end{bmatrix}, \quad D_c = D_c^d. \quad (16d)$$

Note that the above expressions are for the SISO case. The corresponding DT stochastic state space model is

$$\mathbf{x}_{k+1} = A\mathbf{x}_k + B\mathbf{u}_k + G\mathbf{w}_k, \quad (17a)$$

$$\mathbf{z}_k = C\mathbf{x}_k + D\mathbf{u}_k. \quad (17b)$$

B. Reference tracking and input regularization objectives

Define the output and input reference tracking error $\bar{z}(t)$ as

$$\bar{z}(t) = \begin{bmatrix} z(t) - \bar{z}(t) \\ u(t) - \bar{u}(t) \end{bmatrix} = \begin{bmatrix} z(t) - \bar{z}_k \\ u(t) - \bar{u}_k \end{bmatrix}, \quad \text{for } t_k \leq t < t_{k+1}, \quad (18)$$

where we consider piece-wise constant parameterization on references $\bar{z}(t) = \bar{z}_k$ and $\bar{u}(t) = \bar{u}_k$ for $t_k \leq t < t_{k+1}$.

We then can define the following CT LQ-OCP for minimizing the output and input reference tracking error as

$$\min_{x, u, z, \bar{z}} \phi_z + \phi_u = \int_{t_0}^{t_0+T} l_{\bar{z}}(\bar{z}(t)) dt \quad (19a)$$

$$\text{s.t. } \mathbf{x}(t_0) = \hat{x}_0, \quad (1c), \quad (9a), \quad (10), \quad (18), \quad (19b)$$

with the stage cost function $l_{\bar{z}}(\bar{z}(t))$

$$l_{\bar{z}}(\bar{z}(t)) = \frac{1}{2} \|W_{\bar{z}} \bar{z}(t)\|_2^2 = \frac{1}{2} \bar{z}(t)' Q_{c\bar{z}} \bar{z}(t), \quad (20)$$

where $Q_{c\bar{z}} = \text{diag}(Q_{cz}, Q_{cu}) = W_{\bar{z}}' W_{\bar{z}}$. Q_{cz} and Q_{cu} are weight matrices for the reference tracking and input regularization objectives.

The above problem is in CT and subject to a linear deterministic time-delay system. The corresponding DT equivalent of (19) is

$$\min_{x, u} \phi_z + \phi_u = \sum_{k \in \mathcal{N}} l_{\bar{z},k}(x_k, u_k) \quad (21a)$$

$$\text{s.t. } x_0 = \hat{x}_0, \quad (11a), \quad (15), \quad (21b)$$

with the stage cost function $l_{\bar{z},k}(x_k, u_k)$

$$l_{\bar{z},k}(x_k, u_k) = \frac{1}{2} \begin{bmatrix} x_k \\ u_k \end{bmatrix}' Q \begin{bmatrix} x_k \\ u_k \end{bmatrix} + q_k' \begin{bmatrix} x_k \\ u_k \end{bmatrix} + \rho_k, \quad (22)$$

where

$$q_k = M[\bar{z}_k; \bar{u}_k], \quad \rho_k = \frac{1}{2} \begin{bmatrix} \bar{z}_k \\ \bar{u}_k \end{bmatrix}' Q_{c\bar{z}} \begin{bmatrix} \bar{z}_k \\ \bar{u}_k \end{bmatrix} T_s, \quad k \in \mathcal{N}. \quad (23)$$

Note that when using NS state space realization, the reference trajectory becomes $\bar{z}_{k+j} = \bar{z}(t) - \hat{z}_{k+j|k}^s$ for $t \in [t_{k+j}, t_{k+j+1})$.

Remark 2 The studies [22], [23] described the discrete system matrices (A, B, Q, M) as differential equations and proposed a novel step-doubling method for solving them. Their numerical experiments showed that the proposed numerical method is significantly faster than the standard ODE method while keeping the same accuracy.

Note that $u = [u_0; u_1; \dots; u_{N-1}]$ and $u_k = I_k u$ for $I_k = [0 \dots I \dots 0]$ and $k \in \mathcal{N}$. The system state x_k can be expressed as

$$x_k = b_k + \Gamma_k u, \quad b_k = A^k x_0, \quad \Gamma_k = \sum_{i=0}^k A^{k-1-i} B I_i. \quad (24)$$

We then rewrite the LQ-OCP (21) in the form of QP

$$\phi_z + \phi_u = \frac{1}{2} u' H_{\bar{z}} u + g_{\bar{z}}' u, \quad (25)$$

where

$$H_{\bar{z}} = \sum_{k=0}^{N-1} \begin{bmatrix} \Gamma_k \\ I_k \end{bmatrix}' Q \begin{bmatrix} \Gamma_k \\ I_k \end{bmatrix}, \quad g_{\bar{z}} = \sum_{k=0}^{N-1} \begin{bmatrix} \Gamma_k \\ I_k \end{bmatrix}' \left(Q \begin{bmatrix} b_k \\ 0 \end{bmatrix} + q_k \right). \quad (26)$$

C. Input ROM and economic objectives

We then consider the LQ-OCP for penalizing the input rate-of-movement (ROM) and input cost (economic)

$$\phi_{\Delta u} + \phi_{eco} = \int_{t_0}^{t_0+T} l_{\bar{u}}(\dot{u}(t), u(t)) dt, \quad (27)$$

and the stage cost function is

$$l_{\bar{u}}(\dot{u}(t), u(t)) = \frac{1}{2} \|W_{c\Delta u} \dot{u}(t)\|_2^2 + q_{ceco}' u(t), \quad (28)$$

where $Q_{c\Delta u} = W_{c\Delta u}' W_{c\Delta u}$ and q_{ceco} are the weight matrices of the input ROM and the economic objectives.

The discretization of the input cost objective is intuitive if a zero-order hold (ZOH) parameterization is applied to the inputs. However, this is not the case for the input ROM objective function, as the input derivative is not even defined. The previous work [7] described the discretization schemes on the input ROM penalty function using piece-wise affine functions and the ZOH discretization. The author approved that the solution of the discrete problem is convergent in L^2 towards the original problem's minimizers. When taking the number of the discretization $N \rightarrow \infty$, the minimizers of the discrete problem converge in H^1 towards the solution of the original problem.

Lets consider the ZOH discretization on the input $u(t) = u_k$ for $t \in [t_k, t_{k+1})$ and the discrete approximation of the input ROM penalty is

$$\phi_{\Delta u} = \frac{1}{T_s} \sum_{k \in \mathcal{N}} \|u_k - u_{k-1}\|_{Q_{c\Delta u}}^2. \quad (29)$$

We then can perform the discretization of (27) as

$$\phi_{\Delta u} + \phi_{eco} = \sum_{k \in \mathcal{N}} l_{\bar{u},k}(u_k, u_{k-1}), \quad (30)$$

with the stage cost function

$$l_{\bar{u},k}(u_k, u_{k-1}) = \frac{1}{2} \begin{bmatrix} u_k \\ u_{k-1} \end{bmatrix}' \bar{Q}_{\Delta u} \begin{bmatrix} u_k \\ u_{k-1} \end{bmatrix} + q_{eco}' u_k, \quad (31)$$

where u_{-1} indicates the input at t_{0-1} . The discrete-time weights $\bar{Q}_{\Delta u}$ and q_{eco} are

$$\bar{Q}_{\Delta u} = \begin{bmatrix} Q_{\Delta u} & -Q_{\Delta u} \\ -Q_{\Delta u} & Q_{\Delta u} \end{bmatrix}, \quad Q_{\Delta u} = \frac{Q_{c\Delta u}}{T_s}, \quad q_{eco} = q_{ceco} T_s. \quad (32)$$

Consequently, along with possible input box and input ROM constraints, we can express the input ROM and economic objective functions in the form of QP as

$$\min_u \phi_{\Delta u} + \phi_u = \frac{1}{2} u' H_{\bar{u}} u + g_{\bar{u}}' u \quad (33a)$$

$$\text{s.t. } u_{\min,k} \leq u_k \leq u_{\max,k}, \quad k \in \mathcal{N}, \quad (33b)$$

$$\Delta u_{\min,k} \leq \Delta u_k \leq \Delta u_{\max,k}, \quad k \in \mathcal{N}, \quad (33c)$$

where the quadratic and linear term coefficients

$$H_{\bar{u}} = \sum_{k=1}^{N-1} \begin{bmatrix} I_k \\ I_{k-1} \end{bmatrix}' \bar{Q}_{\Delta u} \begin{bmatrix} I_k \\ I_{k-1} \end{bmatrix} + I_0' Q_{\Delta u} I_0, \quad (34a)$$

$$g_{\bar{u}} = \sum_{k=0}^{N-1} -I_0' Q_{\Delta u} u_{-1} + I_k' q_{eco}. \quad (34b)$$

D. Soft output constraint penalty

We then introduce the soft output constraints

$$z_{k+j|k} \geq z_{\min, k+j|k} - \xi_{k+j}, \quad k = 1, 2, \dots, N, \quad (35a)$$

$$z_{k+j|k} \leq z_{\max, k+j|k} + \eta_{k+j}, \quad k = 1, 2, \dots, N, \quad (35b)$$

$$\xi_{k+j} \geq 0, \quad k = 1, 2, \dots, N, \quad (35c)$$

$$\eta_{k+j} \geq 0, \quad k = 1, 2, \dots, N, \quad (35d)$$

where ξ and η are slackness variables. The output z_k is subject to the deterministic system (11). $z_{\min, k+j|k} = z_{\min, k+j} - \hat{z}_{k+j|k}^s$ and $z_{\max, k+j|k} = z_{\max, k+j} - \hat{z}_{k+j|k}^s$ are modified soft constraints.

The corresponding penalty function

$$\phi_{\xi} + \phi_{\eta} = \int_{t_0}^{t_0+T} l_{\xi}(\xi(t)) + l_{\eta}(\eta(t)) dt, \quad (36)$$

with the stage cost functions

$$l_{\xi}(\xi(t)) = \frac{1}{2} \|W_{c\xi} \xi(t)\|_2^2 + q'_{c\xi} \xi(t), \quad (37)$$

$$l_{\eta}(\eta(t)) = \frac{1}{2} \|W_{c\eta} \eta(t)\|_2^2 + q'_{c\eta} \eta(t), \quad (38)$$

where $Q_{c\xi} = W'_{c\xi} W_{c\xi}$, $Q_{c\eta} = W'_{c\eta} W_{c\eta}$, $q_{c\xi}$ and $q_{c\eta}$ are weight matrices of the quadratic and linear penalty functions, respectively. We assume piece-wise constant $\xi(t) = \xi_k$ and $\eta(t) = \eta_k$ for $t \in [t_k, t_k + T_s)$. The corresponding discrete equivalent is

$$\phi_{\xi} + \phi_{\eta} = \sum_{k=1}^N \frac{1}{2} (\|\xi_k\|_{Q_{\xi}}^2 + \|\eta_k\|_{Q_{\eta}}^2) + q'_{\xi} \xi_k + q'_{\eta} \eta_k, \quad (39)$$

where $Q_{\xi} = T_s Q_{c\xi}$, $q_{\xi} = T_s q_{c\xi}$, $Q_{\eta} = T_s Q_{c\eta}$ and $q_{\eta} = T_s q_{c\eta}$.

The DT penalty functions (39) can be rewritten in the form of QP as

$$\phi_{\xi} + \phi_{\eta} = \frac{1}{2} \begin{bmatrix} \xi \\ \eta \end{bmatrix}' H_{\bar{s}} \begin{bmatrix} \xi \\ \eta \end{bmatrix} + g'_{\bar{s}} \begin{bmatrix} \xi \\ \eta \end{bmatrix}, \quad (40a)$$

where $\xi = [\xi_1; \xi_2; \dots; \xi_N]$ and $\eta = [\eta_1; \eta_2; \dots; \eta_N]$ and

$$H_{\xi} = \text{diag}(Q_{\xi}; Q_{\xi}; \dots; Q_{\xi}), \quad g_{\xi} = [q_{\xi} \quad q_{\xi} \quad \dots \quad q_{\xi}]', \quad (41a)$$

$$H_{\eta} = \text{diag}(Q_{\eta}; Q_{\eta}; \dots; Q_{\eta}), \quad g_{\eta} = [q_{\eta} \quad q_{\eta} \quad \dots \quad q_{\eta}]', \quad (41b)$$

$$H_{\bar{s}} = \text{diag}(H_{\xi}; H_{\eta}), \quad g_{\bar{s}} = [g_{\xi} \quad g_{\eta}]'. \quad (41c)$$

E. Design and implementation of CT-LMPC

Combining the objective functions introduced previously, we have

$$\min_{\{u, \xi, \eta\}} \phi = \phi_z + \phi_u + \phi_{\Delta u} + \phi_{eco} + \phi_{\xi} + \phi_{\eta} \quad (42a)$$

$$s.t. \quad x_0 = \hat{x}_0, \quad (11a), \quad (33b), \quad (33c), \quad (35), \quad (42b)$$

Algorithm 1 Design of CT-LMPC

Require: ($G(s), H(s), Q_{c\bar{z}}, Q_{c\Delta u}, Q_{c\xi}, Q_{c\eta}, q_{ceco}, q_{c\xi}, q_{c\eta}, R_{vv}, N, T_s$)

Compute NS state space matrices $\mathcal{G}_c, \mathcal{H}_c, \mathcal{G}_d$ and \mathcal{H}_d using (9) and (11)

Compute Kalman gain K_{fx} using (14)

Compute DT weight matrices Q and M using (22)

Compute $b = \{b_k\}$ and $\Gamma = \{\Gamma_k\}$ for $k \in \mathcal{N}$ using (24)

Compute $H_{\bar{z}}$ of ϕ_z and ϕ_u using (26)

Compute $H_{\bar{u}}$ of $\phi_{\Delta u}$ and ϕ_{eco} using (34a)

Compute $H_{\bar{s}}$ and $g_{\bar{s}}$ of ϕ_{ξ} and ϕ_{η} using (40)

Set $H = \text{diag}([H_{\bar{z}} + H_{\bar{u}}; H_{\bar{s}}])$

Return: ($\mathcal{G}_d, \mathcal{H}_d, K_{fx}, Q, M, b, \Gamma, H, g_{\bar{s}}$)

Algorithm 2 Implementation of CT-LMPC

Require: ($\bar{z}, \bar{u}, u_{\min}, u_{\max}, \Delta u_{\min}, \Delta u_{\max}, z_{\min}, z_{\max}, u_{k-1}, y_k, \hat{x}_{k-1|k-1}^s, \mathcal{G}_d, \mathcal{H}_d, K_{fx}, Q, M, b, \Gamma, H, g_{\bar{s}}$)

Run Kalman filter for $\hat{x}_{k|k}^s$ and $\{\hat{z}_{k+j|k}^s\}$ using (15b)

for $j=1, 2, \dots, N$ **do**

Update $\bar{z}_{k+j}, z_{\min, k+j}$ and $z_{\max, k+j}$ with $\hat{z}_{k+j|k}^s$

Set $q_{k+j} = M[\bar{z}_{k+j}; \bar{u}_{k+j}]$

end for

Compute $g_{\bar{z}}$ using (26)

Compute $g_{\bar{u}}$ using (34b)

Set $g = [g_{\bar{z}} + g_{\bar{u}}; g_{\bar{s}}]$

Solve the QP (42) to get the optimal solution u^*

Let $u_k \leftarrow u^*(1 : n_u)$

Return: ($u_k, \hat{x}_{k|k}^s$)

where the objective functions $\phi_z, \phi_u, \phi_{\Delta u}, \phi_{eco}, \phi_{\xi}$ and ϕ_{η} are the corresponding discrete equivalent of their original CT LQ-OCPs.

The cost function ϕ can be expressed in the form of QP as

$$\phi = \frac{1}{2} \begin{bmatrix} u \\ \xi \\ \eta \end{bmatrix}' H \begin{bmatrix} u \\ \xi \\ \eta \end{bmatrix} + g' \begin{bmatrix} u \\ \xi \\ \eta \end{bmatrix}, \quad (43)$$

where

$$H = \begin{bmatrix} H_{\bar{z}} + H_{\bar{u}} & 0 \\ 0 & H_{\bar{s}} \end{bmatrix}, \quad g = \begin{bmatrix} g_{\bar{z}} + g_{\bar{u}} \\ g_{\bar{s}} \end{bmatrix}. \quad (44)$$

Consequently, we obtain the objective function (42) that is the discrete-time equivalent of the CT LQ-OCPs introduced in previous subsections. Algorithm 1 describes the design of CT-LMPC and the implementation of the CT-LMPC is illustrated by Algorithm 2.

III. NUMERICAL EXPERIMENTS

This section describes closed-loop simulations with the proposed CT-LMPC and standard DT-LMPC. Consider the

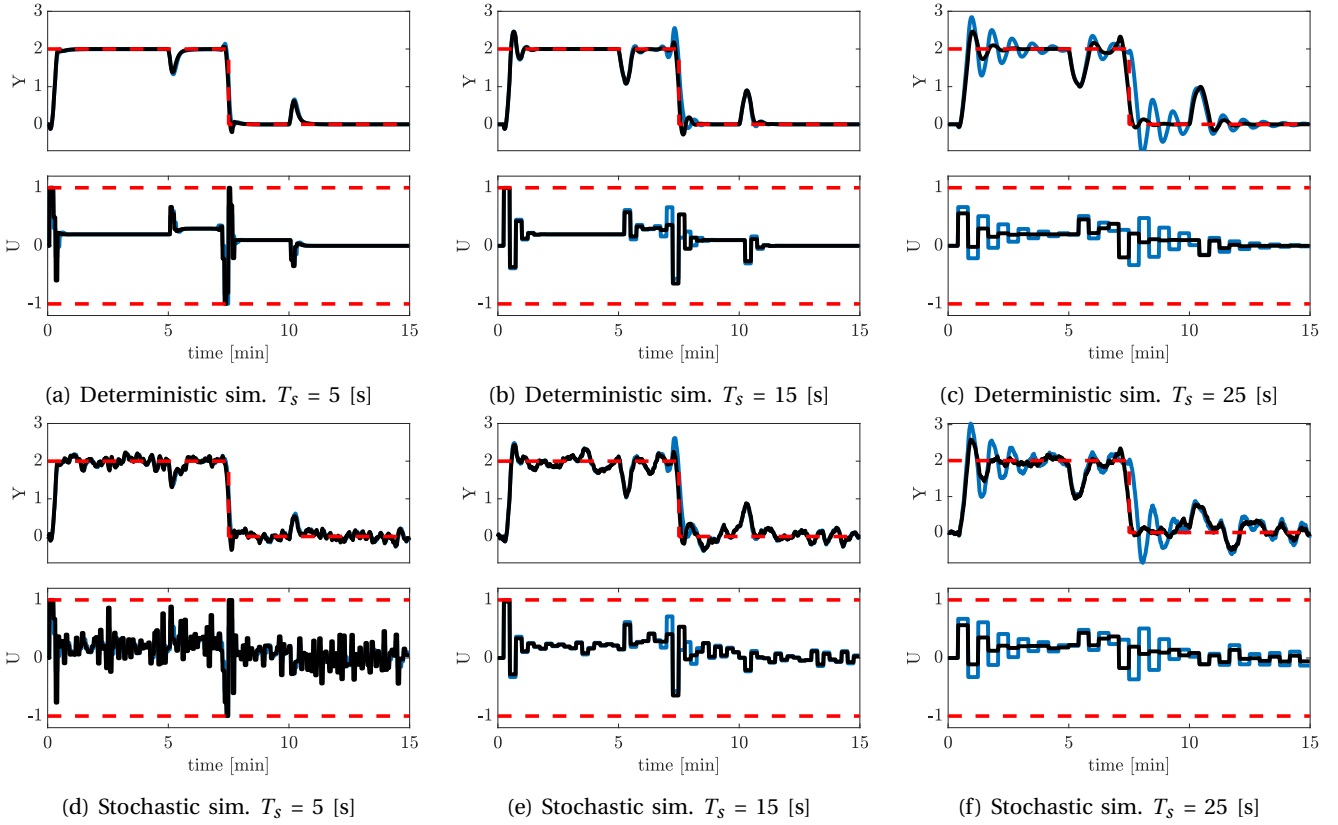


Fig. 1: SISO example closed-loop simulations with different controller sampling times $T_s^c = 5, 15, 25$ [s]. The blue curves indicate the results obtained from DT-LMPC and the black curves are the results of CT-LMPC.

simulation model with the following expressions

$$\mathbf{Z}(s) = G(s)U(s) + G_d(s)(D(s) + \mathbf{W}(s)), \quad (45a)$$

$$\mathbf{Y}(s) = \mathbf{Z}(s) + \mathbf{V}(s), \quad (45b)$$

and it can be converted to a state space model with the sampling time T_s as

$$\mathbf{x}_{k+1} = \mathbf{A}\mathbf{x}_k + \mathbf{B}u_k + \mathbf{E}d_k + \mathbf{G}\mathbf{w}_k, \quad \mathbf{w}_k \sim N_{iid}(0, R_{ww}), \quad (46a)$$

$$\mathbf{y}_k = \mathbf{C}\mathbf{x}_k + \mathbf{D}u_k + \mathbf{v}_k, \quad \mathbf{v}_k \sim N_{iid}(0, R_{vv}), \quad (46b)$$

where $x_k \sim N(\hat{x}_k, P)$ is the states, u_k is the inputs and d_k is the disturbance.

In the closed-loop simulations, we use (46) as the simulator. We develop the DT-LMPC based on the previous work by [8]. We estimate the control model (6) for CT- and DT-LMPC by step-response experiments. It may be done using system parameters identification schemes introduced by [10], [11], [15].

A. Closed-loop simulation - a SISO example

In the following, we perform a series of closed-loop simulations with CT- and DT-LMPC implementations for a SISO system. The SISO example considers the simulation model (45) with transfer functions

$$g(s) = \frac{10.12(-3.41s + 1)}{(15.9s + 1)(24.2s + 1)}, \quad (47a)$$

$$g_d(s) = \frac{-0.5}{(5.8s + 1)(4.7s + 1)}, \quad (47b)$$

and we convert the transfer functions into the DT state space (46) with sampling time $T_s = 1$ [s]. The unknown disturbance $d_k = 2.0$ for $3.75 \leq t \leq 11.25$ [min]. The system covariances are $R_{ww} = R_{vv} = 0.05^2$.

The estimated control model (6) for the two MPCs is

$$\hat{g}(s) = \frac{10.12(-3.58s + 1)}{(18.9s + 1)(22.2s + 1)}, \quad \hat{h}(s) = \frac{1}{s} \frac{0.6}{s + 1}, \quad (48)$$

where we select $\hat{h}(s)$ as an integrator to ensure the controller can handle step-type error [14], [18].

In the SISO example, we consider the objective function (42) with only the reference tracking ϕ_z and input ROM $\phi_{\Delta u}$ cost functions. For DT-LMPC, ϕ_z and $\phi_{\Delta u}$ are designed as

$$\phi = \sum_{k=0}^{N-1} \|z_{k+1} - \bar{z}_{k+1}\|_{Q_{cz}}^2 + \|u_k - u_{k-1}\|_{Q_{c\Delta u}}^2, \quad (49)$$

The prediction and control horizon is $N = 20$. The output target is $\bar{z} = 2$ for $t \leq 7.5$ [min]. The weight matrices of the two objectives are $Q_{cz} = 20$ and $Q_{c\Delta u} = 1$, and the input constraints are $u_{\min} = -1$ and $u_{\max} = 1$.

To demonstrate the contrast between CT- and DT-LMPC, we discretize both using different controller sampling times $T_s^c = 5, 15, 25$ [s]. Fig. 1 shows closed-loop simulations of the SISO system with CT- and DT-LMPC implementations. In Fig. 1a and 1d, both CT-LMPC (black curves) and DT-LMPC (blue curves) effectively control the

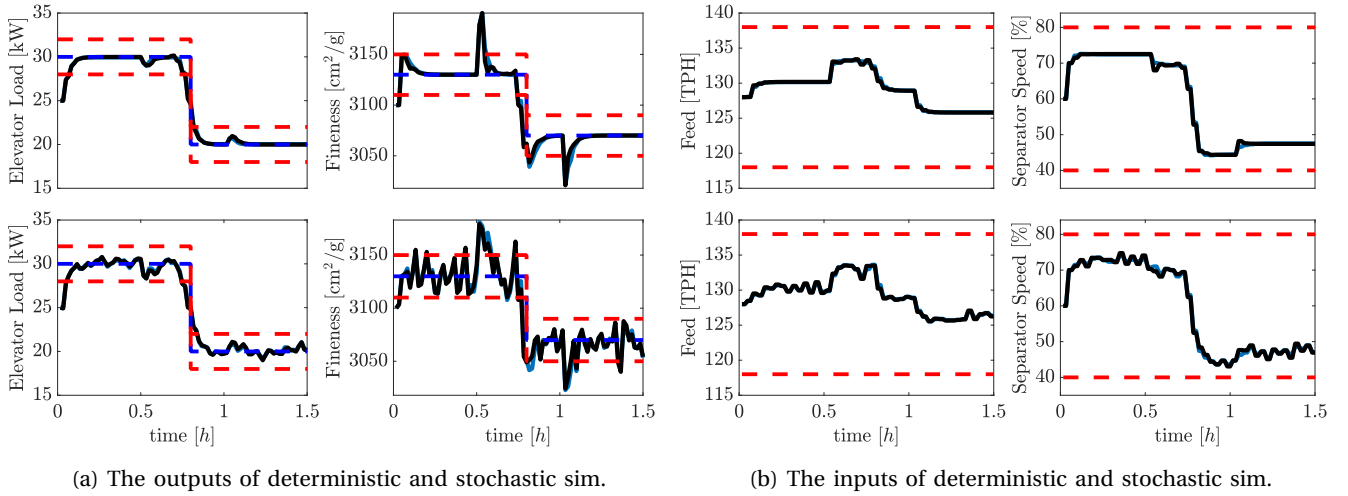


Fig. 2: The closed-loop simulations of a simulated cement mill system with DT-LMPC (blue curves) and CT-LMPC (black curves) implementations. The simulator and controller sampling times are $T_s = 1$ [min] and $T_s^c = 2$ [min]

SISO system, allowing the outputs to track the given target (red dashed line). Two overshoots occur at $t = 3.75$ and 11.25 [min] due to an unknown disturbance, and the two MPCs can handle it after a few iterations. In this case, the simulation results show little difference between the two MPCs. Upon increasing T_s^c to 15 [s], additional overshoots emerge around 1 and 7.5 [min] in Fig. 1b and 1e. Notably, the second overshoot at $t = 7.5$ [min] for DT-LMPC is larger than that for CT-LMPC. Moreover, the overshoots resulting from the unknown disturbance are more significant compared to the previous scenario, yet both MPCs can manage it. Fig. 1c and 1f show the closed-loop simulations when $T_s^c = 25$ [s]. Here, we can see a significant decrease in the closed-loop performance of both MPCs compared to the previous two cases. Both CT- and DT-LMPC exhibit oscillations and struggle to follow the target. However, the amplitude of the output from CT-LMPC is considerably smaller than that from DT-LMPC. CT-LMPC maintains control of the output to the desired target after 1-2 iterations, while DT-LMPC fails to do so.

The SISO example simulation results show that a large sampling time can degrade the closed-loop performance of the predictive controller and even lead to system instability. For the same system parameters, the proposed CT-LMPC has a better closed-loop performance than the traditional DT-LMPC, and this gap will increase with the increase of the sampling time.

B. Closed loop simulation - a MIMO example

The MIMO example concerns the cement mill system introduced in [15], [19], where the cement mill system is described by transfer functions

$$G(s) = \begin{bmatrix} \frac{0.62e^{-5s}}{(45s+1)(8s+1)} & \frac{0.29(8s+1)e^{-1.5s}}{(2s+1)(38s+1)} \\ \frac{-15e^{-5s}}{60s+1} & \frac{5e^{-0.1s}}{(14s+1)(s+1)} \end{bmatrix}, \quad (50a)$$

$$G_d(s) = \begin{bmatrix} \frac{-1.0e^{-3s}}{(32s+1)(21s+1)} \\ \frac{60}{(30s+1)(20s+1)} \end{bmatrix}. \quad (50b)$$

The system inputs $u =$ [feed flow rate (TPH); separator speed (%)] and the system outputs $z =$ [elevator load (kW); fineness (cm^2/g)]. The system disturbance D is the clinker hardness (HGI). The transfer functions of the estimated control model (6) for the two MPCs are

$$\hat{G}(s) = \begin{bmatrix} \frac{0.8e^{-4s}}{(30s+1)(15s+1)} & \frac{-0.45e^{-2s}}{30.0s+1} \\ \frac{-17.7e^{-3s}}{(65s+1)(15s+1)} & \frac{-19.4}{15s+1} \end{bmatrix}, \quad (51a)$$

$$\hat{H}(s) = \text{diag} \left(\left[\frac{1}{s} \frac{0.5}{s+1}; \frac{1}{s} \frac{1}{s+1} \right] \right), \quad (51b)$$

where we manually introduce the plant-model mismatch on the deterministic model $\hat{G}(s)$.

The cement mill system is converted into a DT state space model (46) with the sampling time $T_s = 1$ [min]. The simulation time $T_{sim} = 1.5$ [h]. The related covariances are selected as $R_{ww} = 1.0$ and $R_{yy} = \text{diag}([0.1; 50])$. The unknown disturbance $d_k = 8$ for 0[min] and $d_k = 0$ for the rest of the time.

For the CT- and DT-LMPC, the controller sampling time $T_s^c = 2$ [min], the prediction and control horizon is $N = 60$. The weight matrices for the reference tracking, input ROM, economics and soft output constraints penalty are $Q_{cz} = \text{diag}(200, 10)$, $Q_{c\Delta u} = \text{diag}(2, 1)$, $q_{ceco} = [2; 1]$, $Q_{c\xi} = Q_{c\eta} = \text{diag}(2000, 100)$ and $q_{c\xi} = q_{c\eta} = [20; 1]$, respectively. The input hard constraints are $u_{\min} = [-10; -20]$, $u_{\max} = [10; 20]$, $\Delta u_{\min} = [-5; -10]$ and $\Delta u_{\max} = [5; 10]$. The soft output constraints $z_{\min} = [-2; -20]$ and $z_{\max} = [2; 20]$ and are deviation variables.

Fig. 2 illustrates the closed-loop simulations of a simulated cement mill system with CT- and DT-LMPC implementations. In Fig. 2a, both CT-LMPC (black curves) and DT-LMPC (blue curves) can regulate the outputs towards the desired targets (blue dashed lines) and within the given bounds for most of the time. An overshoot, attributed to the plant-model mismatch in y_2 (Fineness), is observed. The two predictive controllers can handle the problem and bring the output back to the target after a

few iterations. At $t = 0.5$ and 1.5 hours, two overshoots on the output occur due to the unknown disturbance. Both CT- and DT-LMPC can reject the unknown disturbance. Additionally, an overshoot arises at around $t = 0.75$ [h] on the Fineness due to a step change in the output targets. DT-LMPC exhibits a slightly larger overshoot than CT-LMPC.

The MIMO example closed-loop simulations show that the proposed CT-LMPC and DT-LMPC exhibit highly similar closed-loop performance. They even converge to identical optimal solutions when using appropriate sampling time and tuning parameters. This outcome aligns with the earlier SISO example presented in Fig. 1a and 1d, reinforcing the consistency of our findings.

IV. CONCLUSIONS

This paper presents the design, discretization and implementation of CT-LMPC. We introduce different objective functions of CT-LMPC and show their discretization and implementation. From the numerical experiments, we notice that the proposed CT-LMPC has the following features:

1. When using an appropriate sampling time and well-tuned weight matrices, the proposed CT-LMPC has a highly similar control performance as the traditional DT-LMPC, and they will converge to an identical (very similar) optimal solution
2. The proposed CT-LMPC has a better closed-loop performance than the traditional DT-LMPC when the controller sampling time is large. This gap will increase with the increase in controller sampling time

REFERENCES

- [1] W. Alt, C. Schneider, and M. Seydenschwanz, "Regularization and implicit euler discretization of linear-quadratic optimal control problems with bang-bang solutions," *Applied Mathematics and Computation*, vol. 287-288, pp. 104-124, 2016.
- [2] K. J. Åström, *Introduction to stochastic control theory*. Academic Press New York, 1970.
- [3] K. J. Åström and B. Wittenmark, *Computer-Controlled Systems: Theory and Design, Third Edition*, ser. Dover Books on Electrical Engineering. Dover Publications, 2011.
- [4] M. Cannon and B. Kouvaritakis, "Infinite horizon predictive control of constrained continuous-time linear systems," *Automatica*, vol. 36, no. 7, pp. 943-955, 2000.
- [5] G. F. Franklin, J. D. Powell, and M. L. Workman, *Digital Control of Dynamic Systems*, 2nd ed., ser. Electrical and Computer Engineering; Control Engineering. Reading Massachusetts: Addison-Wesley, 1990.
- [6] G. Frison and J. B. Jørgensen, "Efficient implementation of the riccati recursion for solving linear-quadratic control problems," in *2013 IEEE International Conference on Control Applications (CCA)*, 2013, pp. 1117-1122.
- [7] M. Hagdrup, "Model predictive control for systems described by stochastic differential equations," Ph.D. dissertation, Technical University of Denmark, Kgs. Lyngby, Denmark, 2019.
- [8] M. Hagdrup, D. Boiroux, Z. Mahmoudi, H. Madsen, N. Kjølstad Poulsen, B. Poulsen, and J. B. Jørgensen, "On the significance of the noise model for the performance of a linear MPC in closed-loop operation," *IFAC-PapersOnLine*, vol. 49, no. 7, pp. 171-176, 2016, 11th IFAC Symposium on Dynamics and Control of Process Systems Including Biosystems DYCOPS-CAB 2016.
- [9] W. W. Hager, "Runge-kutta methods in optimal control and the transformed adjoint system," *Numerische Mathematik*, vol. 87, pp. 247-282, 2000.
- [10] J. B. Jørgensen and S. B. Jørgensen, "Comparison of Prediction-Error-Modelling Criteria," in *2007 American Control Conference*, 2007, pp. 140-146.
- [11] —, "MPC-Relevant Prediction-Error Identification," in *2007 American Control Conference*, 2007, pp. 128-133.
- [12] H. Li and Y. Shi, "Event-triggered robust model predictive control of continuous-time nonlinear systems," *Automatica*, vol. 50, no. 5, pp. 1507-1513, 2014.
- [13] M. M. Morato, J. E. Normey-Rico, and O. Sename, "Model predictive control design for linear parameter varying systems: A survey," *Annual Reviews in Control*, vol. 49, pp. 64-80, 2020.
- [14] K. R. Muske and T. A. Badgwell, "Disturbance modeling for offset-free linear model predictive control," *Journal of Process Control*, vol. 12, no. 5, pp. 617-632, 2002.
- [15] D. H. Olesen, J. K. Huusom, and J. B. Jørgensen, "A tuning procedure for ARX-based MPC of multivariate processes," in *2013 American Control Conference*, 2013, pp. 1721-1726.
- [16] G. Pannocchia, J. B. Rawlings, D. Q. Mayne, and G. M. Mancuso, "Whither discrete time model predictive control?" *IEEE Transactions on Automatic Control*, vol. 60, no. 1, pp. 246-252, 2015.
- [17] G. Pannocchia, J. B. Rawlings, D. Q. Mayne, and W. Marquardt, "On computing solutions to the continuous time constrained linear quadratic regulator," *IEEE Transactions on Automatic Control*, vol. 55, no. 9, pp. 2192-2198, 2010.
- [18] G. Pannocchia and J. Rawlings, "Disturbance models for offset-free model-predictive control," *AIChE Journal*, vol. 49, pp. 426-437, 02 2003.
- [19] G. Prasath, B. Recke, M. Chidambaram, and J. B. Jørgensen, "Application of soft constrained MPC to a cement mill circuit," *IFAC Proceedings Volumes*, vol. 43, no. 5, pp. 302-307, 2010, 9th IFAC Symposium on Dynamics and Control of Process Systems.
- [20] V. Sakizlis, J. Perkins, and E. Pistikopoulos, "Explicit solutions to optimal control problems for constrained continuous-time linear systems," *IEE Proceedings-Control Theory and Applications*, vol. 152, no. 4, pp. 443-452, 2005.
- [21] L. Wang, "Continuous time model predictive control design using orthonormal functions," *International Journal of Control*, vol. 74, no. 16, pp. 1588-1600, 2001.
- [22] Z. Zhang, S. Hørsholt, and J. B. Jørgensen, "Numerical discretization methods for linear quadratic control problems with time delays," in *12th IFAC Symposium on Advanced Control of Chemical Processes (ADCHEM 2024) (accepted)*, 2023.
- [23] Z. Zhang, J. L. Svendsen, M. W. Kaysfeld, A. H. D. Andersen, S. Hørsholt, and J. B. Jørgensen, "Numerical discretization methods for the extended linear quadratic control problem," in *European Control Conference (ECC) 2024 (accepted)*, 2023.